Supplemental Information

# Core-shell nanostructured Zn-Co-O@CoS arrays for high-performance hybrid supercapacitors

Yi He[a], Lei Xie[a], Shixiang Ding[b], Yujia Long[b], Xinyi Zhou[b,*], Qiang Hu[b,*], Dunmin Lin[b,*]

[a]Ecology and Health Institute, Hangzhou Vocational and Technical College, Hangzhou 310018, China

[b]College of Chemistry and Materials Science, Sichuan Normal University, Chengdu 610066, China

## 1. Experimental Section

Treatment of Ni foam (NF): A piece of NF (2 cm × 3 cm) was soaked for 24 h with 0.05 M HCl solution in order to remove the surface oxide layer. The material was taken out and rinsed with acetone, ethanol and deionized water several times in order to remove the oil contamination, respectively. All chemical reagents are analytically pure and used without further refinement.

Synthesis of $ZnO/Co_3O_4$@CoS: 0.02 M $Zn(NO_3)_2 \cdot 6H_2O$, 0.04 M $NH_4F$, and 0.1 M urea were dissolved in 50 mL of DI water under magnetic stirring to form a solution. The reaction solution and NF were subsequently transferred into a 100 mL Teflon-lined stainless-steel autoclave and kept at 120 $^oC$ for 5 h. After cooled to room temperature, the precursors on NF were cleaned with deionized water and ethanol

* Corresponding author: Email: xiniy@foxmail.com (Xinyi Zhou); 18224419800@qq.com (Qiang Hu); ddmd222@sicnu.edu.cn (Dunmin Lin); Fax: +86 28 84760802 Tel: +86 28 84760802

several times. The resultant foam was dried at 60 $^{o}$C for 12 h in a vacuum oven. The precursor was subsequently calcined at 350 $^{o}$C for 2 h at a ramp rate of 2 $^{o}$C $min^{-1}$ under air atmosphere to obtain ZnO. Similarly, adding the mixture of $Co(NO_3)_2 \cdot 6H_2O$ and $Zn(NO_3)_2 \cdot 6H_2O$ can obtain $ZnO/Co_3O_4$ through the same experimental process. The deposition bath (100 mL) contained 10 mM $Co(NO_3)_2 \cdot 6H_2O$ and 0.75 M $CS(NH_2)_2$. The Ag/AgCl was used as the reference electrode, platinum foil was used as the counter electrode, and $ZnO/Co_3O_4$ was used as the working electrode to deposit CoS. The electrochemical deposition of the CoS was performed using the cyclic voltammetry (CV) technology in the potential range from -1.2 to 0.2 V at 5 mV $s^{-1}$ for 30 cycles. The material was taken out and rinsed with deionized water and ethanol several times. The resulting foam was dried at 60 $^{o}$C for 12 h in a vacuum oven. The average mass loading of $ZnO/Co_3O_4$@CoS is about 3 mg $cm^{-2}$.

Materials Characterization: The micromorphology of the samples was observed using scanning electron microscopy (SEM, FEI-Quanta 250, USA) and transmission electron microscope (FE-TEM, GZF20, USA). The elemental analysis of the samples was characterized using a scanning electron microscope (FE-SEM, JSM-7500, Japan) equipped with corresponding energy-dispersive X-ray (EDX) elemental mapping. The crystal structure of the samples was characterized through the X-ray diffraction analysis (XRD, Smart Lab, Riga ku, Japan) with Cu-Kα (λ= 1.540598 Å, Smart Lab) source (scan rate of 4 ° $min^{-1}$) in the 2θ range of 10º~ 80º. The surface element analysis of the samples was carried out by a PHI 5000 VersaProbe XPS instrument (XPS, Thermo ESCALAB 250XI, USA) and Fourier transform infrared spectrum

(FTIR, NICOLET iS50, USA).

Electrochemical Characterization: Electrochemical properties of the electrodes were initially tested in a three-electrode system on an electrochemical workstation (CHI660E, Shanghai, China). The as-prepared samples (1×1 $cm^2$) were used directly as the working Electrodes. Galvanic charge-discharge (GCD), Cyclic voltammetry (CV) and electrochemical impedance spectroscopy (EIS) tests were conducted in 3 M KOH aqueous electrolyte using platinum (Pt) wire as a counter electrode and Hg/HgO as a reference electrode. The specific capacity (C $g^{-1}$) of the electrodes was computed from the GCD curves according to the equation below：

$$Qs = \frac{I\int_0^{\Delta t} Vdt}{m \times \Delta Vmean} = \frac{I\int_0^{\Delta t} Vdt}{m \times \frac{\Delta v}{2}} = 2\frac{I\int_0^{\Delta t} Vdt}{m\Delta V} \quad (1)$$

where $I$, $\Delta t$, $V$, $\Delta V_{mean}$, $m$, and $\Delta V$ are the discharge current (A), discharge time (s), operating potential (V), mean value of operating potential (V), mass (g), and potential window (V) of electroactive materials, respectively.

**Assembly of hybrid supercapacitor device:**

For two-electrode system, the negative electrode was prepared by coating N/O co-doped porous carbon on Ni foam (NOPC/NF) [1]. The NOPC was mixed with poly (vinylidene fluoride) binder (PTFE) and acetylene black at a weight ratio of 7:2:1 in N-methylpyrrolidone (NMP). The paste was coated onto Ni foam (1×1 $cm^2$) and dried at 60 $^oC$ for 12 h in a vacuum oven. Subsequently, the as-formed electrode was pressed into a film under a pressure of 10 MPa. Prior to the assembly of the device, the masses of the positive ($m^+$) and negative electrode materials ($m^-$) were balanced

according to charge balance theory:

$$m+ / m- = C-V- / C+V+ \quad (2)$$

where $m$ is the mass, $C$ is the specific capacity, and $V$ is the voltage range for the positive (+) and negative (−) electrodes.

For the fabrication of ZnO/Co3O4@CoS//NOPC device, the ZnO/$Co_3O_4$@CoS (3 mg in 1×1 $cm^2$) and NOPC (10.7 mg in 1×1 $cm^2$) were used as the positive and negative electrode materials, respectively, and a piece of diaphragm was used as separator to assemble a coin cell in 3 M KOH aqueous electrolyte. The following equations can be used to calculate the specific capacity (C $g^{-1}$), energy density (Wh $kg^{-1}$) and power density (W $kg^{-1}$) of the device from the current charge-discharge curves:

$$Q = 2\frac{I\int_0^{\Delta t} Vdt}{M\Delta V} \quad (3)$$

$$E = \frac{I\int_0^{\Delta t} Vdt}{3.6M} \quad (4)$$

$$P = \frac{3600E}{\Delta t} \quad (5)$$

where $I$, $M$, $\Delta t$, $V$ and $\Delta V$ are the discharge current (A), the total mass of the positive and negative electrode materials (g), discharge time (s), operating voltage (V), and voltage window (V), respectively.

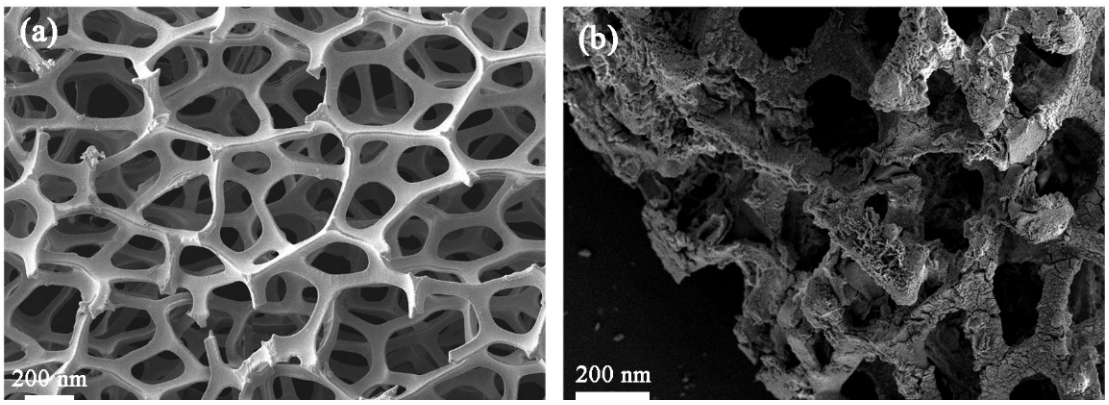


**Fig. S1**. (a-b) SEM images of Ni foam and Zn-Co-O@CoS.

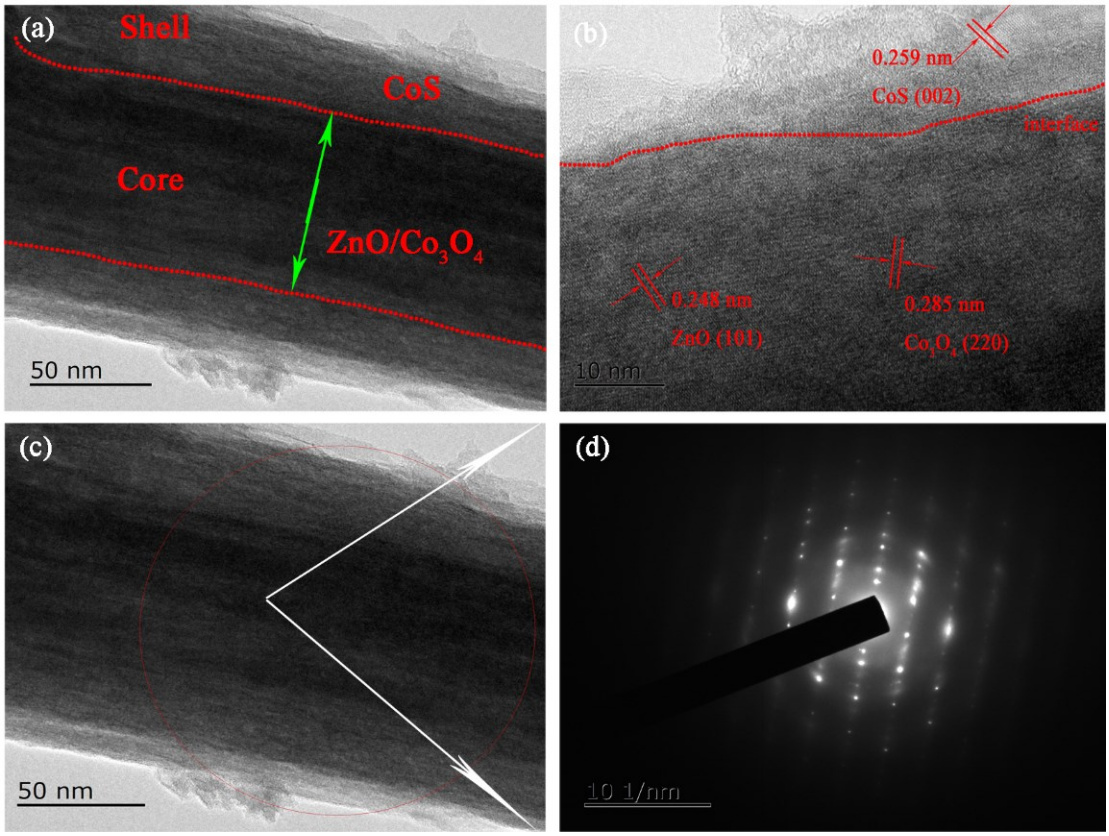


**Fig. S2**. (a) TEM, (b) HRTEM, and (c,d) SAED pattern of as-prepared of Zn-Co-O@CoS.

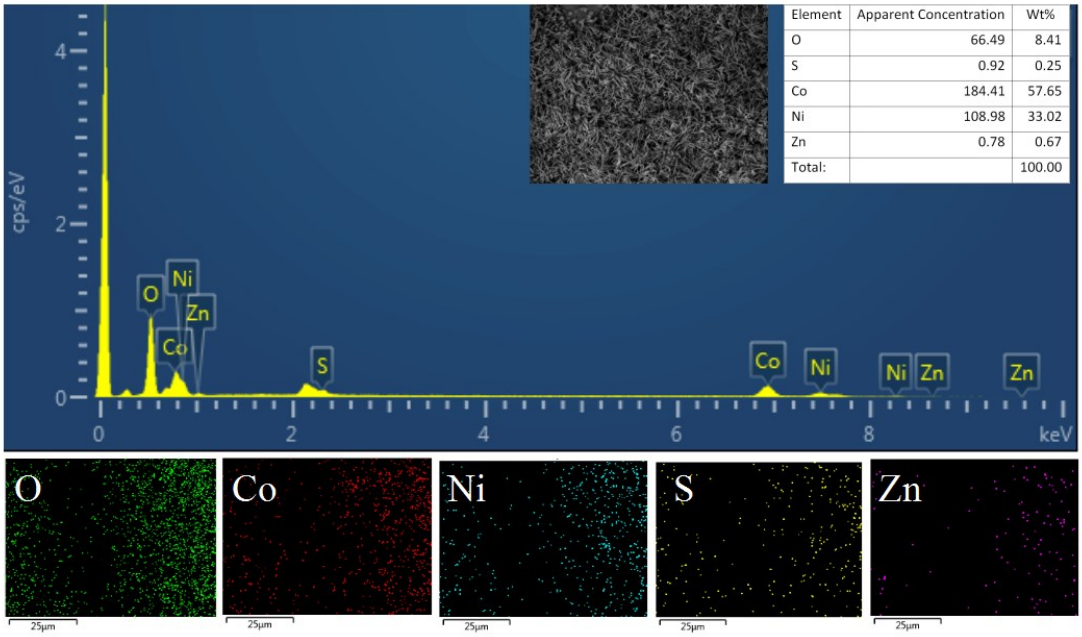


| Element | Apparent Concentration | Wt% |
|---|---|---|
| O | 66.49 | 8.41 |
| S | 0.92 | 0.25 |
| Co | 184.41 | 57.65 |
| Ni | 108.98 | 33.02 |
| Zn | 0.78 | 0.67 |
| Total: | | 100.00 |

**Fig. S3**. Mapping images (Energy dispersive X-ray spectrum) of Zn-Co-O@CoS.

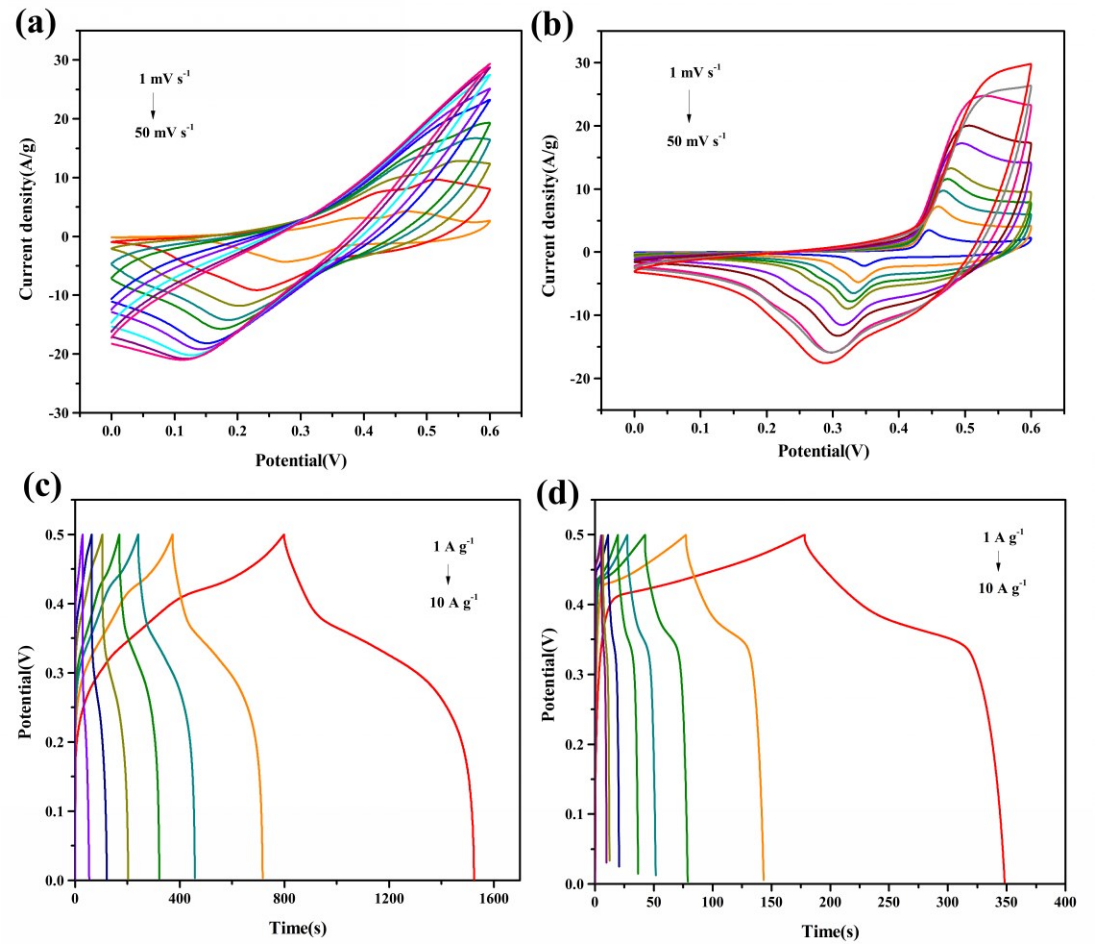


**Fig. S4.** (a-b) CV curves of $ZnO/Co_3O_4$ and ZnO electrodes at different scan rates; (c-d) GCD curves of $ZnO/Co_3O_4$ and ZnO electrodes at different current density.

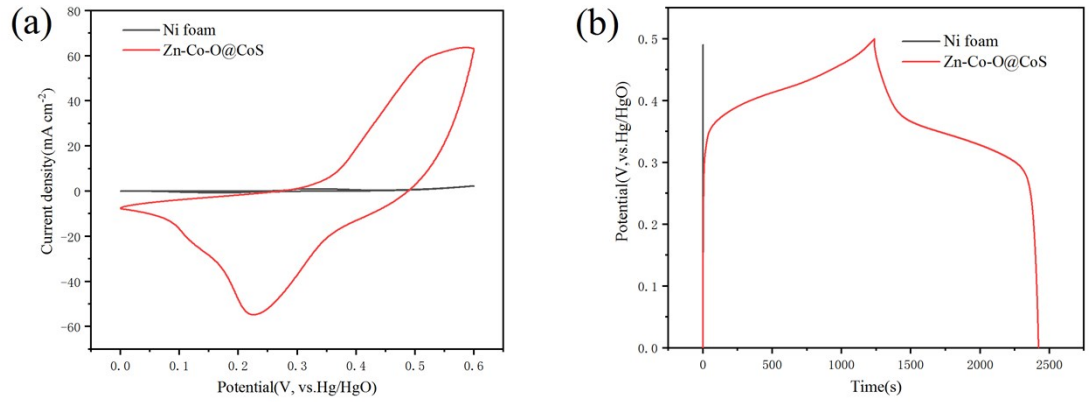


**Fig. S5**. CV and GCD curves of bare Ni foam and Zn-Co-O@CoS electrodes.

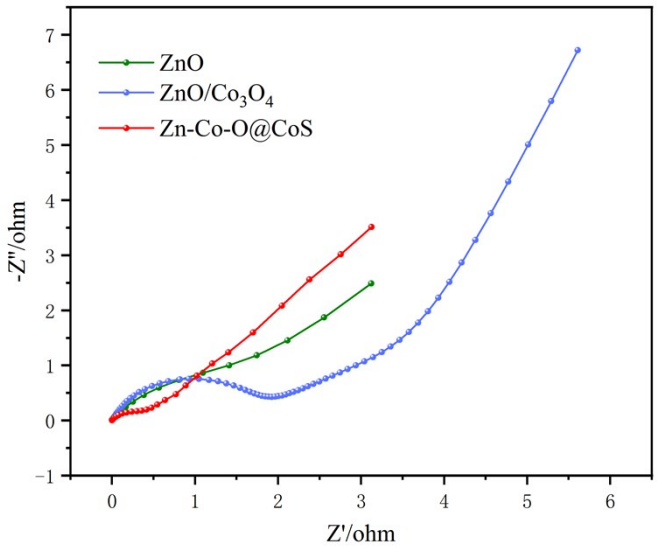


**Fig. S6.** Nyquist low-frequency plots of ZnO, $ZnO/Co_3O_4$ and Zn-Co-O@CoS electrodes.

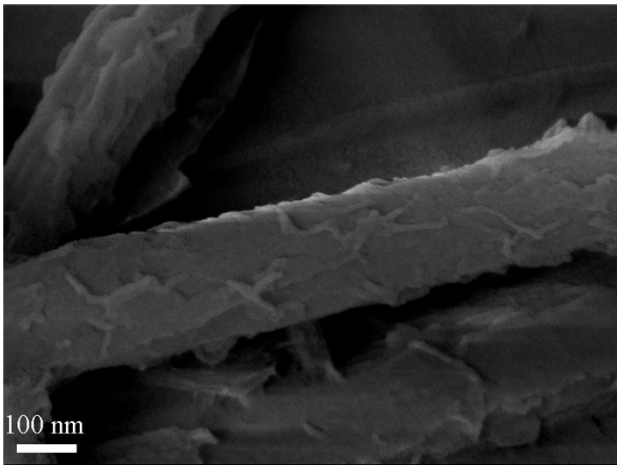


**Fig. S7.** SEM images of Zn-Co-O@CoS electrode after cycling tests.

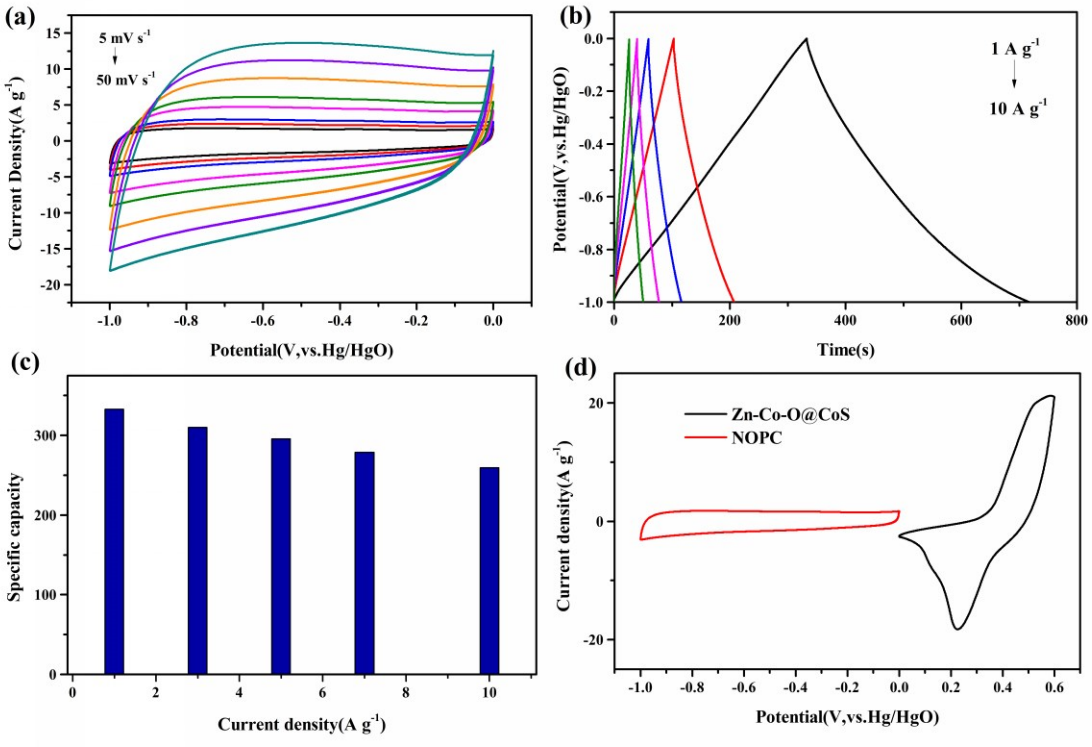


**Fig. S8.** (a) CV curves of NOPC electrode at different scan rates; (b) GCD profiles of NOPC electrode obtained at different current densities; (c) specific capacitance of NOPC electrode; (d) CV curves of NOPC and Zn-Co-O@CoS at a scan rate of 5 mV $s^{-1}$.

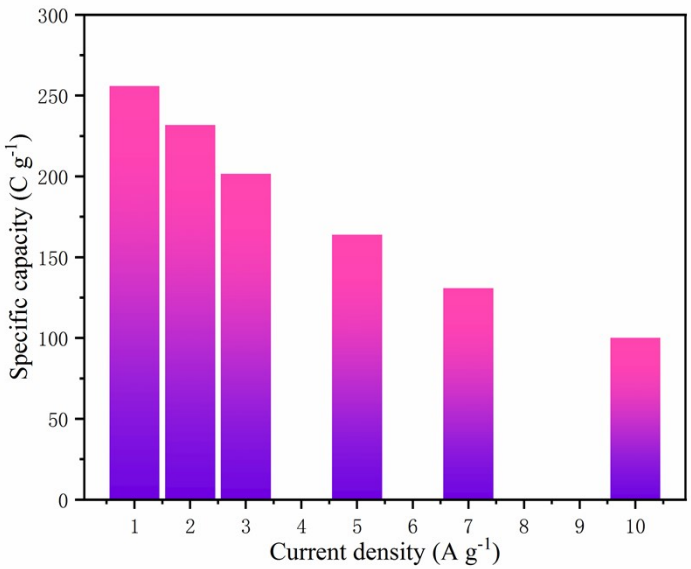


**Fig. S9**. Specific capacity of HSC device at different current densities.

**Table S1.** Comparison of the specific capacities of the reported materials and the Zn-Co-O@CoS.

| Materials | Specific capacity | Current density/scan rate | Ref. |
|---|---|---|---|
| NiO@$Co_3O_4$-NiO | 534.3 F $g^{-1}$ | 4 mA $cm^{-2}$ | 2 |
| α-$MnO_2$@$Co_3O_4$ | 234 F $g^{-1}$ | 0.2 A $g^{-1}$ | 3 |
| $Co_9S_8$@GO | 653 F $g^{-1}$ | 0.5 A $g^{-1}$ | 4 |
| $WO_{3-x}$@Au@$MnO_2$ Core–Shell Nanowires | 588 F $g^{-1}$ | 10 mV $s^{-1}$ | 5 |
| ZIF-8-C@NiAl-LDH | 1370 F $g^{-1}$ | 1 A $g^{-1}$ | 6 |
| ZnO@$MnO_2$ core-shell nanostructure | 423.5 F $g^{-1}$ | 0.5 A $g^{-1}$ | 7 |
| CoAl-LDH/FG-12 | 1222 F $g^{-1}$ | 1 A $g^{-1}$ | 8 |
| NiCoP/NiCo-OH | 1100 F $g^{-1}$ | 1 A $g^{-1}$ | 9 |
| Ni-Al LDH | 1578 F $g^{-1}$ | 1 A $g^{-1}$ | 10 |
| NiAl-LDH nanoplates | 1713 F $g^{-1}$ | 1 A $g^{-1}$ | 11 |
| $KCu_7S_4$@NiMn LDH | 734 F $g^{-1}$ | 1 A $g^{-1}$ | 12 |
| $NiCo_2$Al-LDH | 1137 F $g^{-1}$ | 0.5 A $g^{-1}$ | 13 |
| NiCoP | 1125 F $g^{-1}$ | 1 A $g^{-1}$ | 14 |
| $CoNi_2S_4$ | 1136.5 F $g^{-1}$ | 2 A $g^{-1}$ | 15 |
| Mesoporous $Co_3O_4$ Nanowires | 977 F $g^{-1}$ | 2 A $g^{-1}$ | 16 |

| | | | |
|---|---|---|---|
| Core-shell $MnO_{2-x}$@CoS | 781.1 C $g^{-1}$ | 2 mA $cm^{-2}$ | 17 |
| Core-shell ZnO@CoS | 898.9 C $g^{-1}$ | 3mA $cm^{-2}$ | 18 |
| Zn-Co-O@CoS | 1190 C $g^{-1}$ (2380 F $g^{-1}$) | 1 A $g^{-1}$ | Present work |

## References


[1] Y. Zhou, J. Ren, L. Xia, Q. Zheng, J. Liao, E. Long, F. Xie, C. Xu, D. Lin, Electrochim. Acta, 2018, 284, 336-345.

[2] S. Chandra Sekhar, G. Nagaraju and J. S. Yu, Nano Energy, 2018, 48, 81-92.

[3] Yu D, Yao J, Qiu L, Wang Y, Zhang X, Feng Y, Wang H, J Mater Chem A, 2014 2, 8465-8471.

[4] D. Xiong, X. Li, Z. Bai, J. Li, Y. Han and D. Li, Chemistry-A European Journal, 2018, 10, 2339-2343.

[5] X. Lu, T. Zhai, X. Zhang, Y. Shen, L. Yuan, B. Hu, L. Gong, J. Chen, Y. Gao, J. Zhou, Y. Tong and Z. L. Wang, Advanced Materials, 2012, 24, 938-944.

[6] B. Han, G. Cheng, E. Zhang, L. Zhang and X. Wang, Electrochim. Acta, 2018, 263, 391-399.

[7] M. Huang, F. Li, X. L. Zhao, D. Luo, X.Q. You, Y.X. Zhang, G. Li, Electrochimica Acta, 2015, 152, 172-177.

[8] W. Peng, H. Li and S. Song, ACS Appl. Mater. Interfaces, 2017, 9, 5204-5212.

[9] X. Li, H. Wu, A. M. Elshahawy, L. Wang, S. J. Pennycook, C. Guan and J. Wang, Adv. Funct. Mater, 2018, 28, 1800036.

[10] W. Wang, N. Zhang, Z. Shi, Z. Ye, Q. Gao, M. Zhi and Z. Hong, Chem. Eng. J, 2018, 338, 55-61.

[11] L. Li, K. S. Hui, K. N. Hui, Q. Xia, J. Fu and Y. Cho, J. Alloys Compd, 2017, 721, 803-812.

[12] X. L. Guo, J. M. Zhang, W. N. Xu, C. G. Hu, L. Sun and Y. X. Zhang, J. Mater. Chem. A, 2017, 5, 20579-20587.

[13] X. Gao, X. Liu, D. Wu, B. Qian, Z. Kou, Z. Pan, Y. Pang, L. Miao, J. Wang, Adv. Funct. Mater, 2019, 29, 1903879.

[14] C. Jing, X. Song, K. Li, Y. Zhang, X. Liu, B. Dong, F. Dong, S. Zhao, H. Yao, Y. Zhang, J. Mater. Chem. A, 2020, 8, 1697.

[15] C. Jing, X. Guo, L. Xia, Y. Chen, X. Wang, X. Liu, B. Dong, F. Dong, S. Li, Y. Zhang, Chem. Eng. J, 2020, 379, 122305.

[16] Y. Wang, T. Zhou, K. Jiang, P. Da, Z. Peng, J. Tang, B. Kong, W, Cai, Z. Yang and G. Zheng, Advanced Energy Materials, 2014, 16, 1400696.

[17] Q. Hu, M. Tang, M. He, N. Jiang, C. Xu, D. Lin, Q. Zheng, J. Power Sources, 2020, 446, 227335.

[18] S. Ding, X. Li, X. Jiang, Q. Hu, Y. Yan, Q. Zheng, D. Lin, Electrochimi. Acta, 2020, 354, 136711.